

Characterization of the Vibrational Damping Loss Factor and Viscoelastic Properties of Ethylene–Propylene Rubbers Reinforced with Micro-scale Fillers

G. H. KWAK, K. INOUE, Y. TOMINAGA, S. ASAI, M. SUMITA

Department of Chemistry and Materials Science, Tokyo Institute of Technology, 2-12-1 Ookayama, Meguro-Ku, Tokyo 152-8552, Japan

Received 20 November 2000; accepted 14 March 2001

ABSTRACT: The influence of microscale fillers on ethylene–propylene rubbers (EPR) was examined with respect to their vibrational damping capacity and viscoelastic properties. The vibrational damping and dynamic mechanical properties of reinforced EPR were studied in systematic and comparative ways that reinforced the evidence of a direct relation between the vibrational damping loss factor and its mechanical damping loss factor. In this study, the sensitivity of the vibrational damping loss factor of reinforced EPR was quantified with respect to the variation in thickness, filler type, and filler content. Dynamic mechanical relaxation behaviors were also analyzed. The viscoelastic properties in terms of the storage modulus, loss modulus, mechanical damping loss factor, and frequency dependence of molecular relaxation showed interesting results with the filler types and compositions that had good correspondence with the vibrational damping behaviors. © 2001 John Wiley & Sons, Inc. *J Appl Polym Sci* 82: 3058–3066, 2001

Key words: vibrational damping loss factor; mechanical damping loss factor; viscoelastic properties; glass-relaxation temperature; vapor-grown carbon fibers; reinforcement

INTRODUCTION

Most geometric structures experience vibratory motion, from the world's tallest building to a printed circuit board in a flight-control computer. These unwanted vibrations result in the fatigue and failure of structures, which inevitably cost industries in maintenance, repair, and replacement. Therefore, vibration control is a serious engineering challenge. One of the ways of controlling the noise and vibration in structures is to use passive damping treatments.^{1,2} Passive damping control refers to a structure's ability to damp its

own oscillations as a result of its structural design or material properties or the incorporation of devices, such as coatings and elastomers, that generate energy dissipation.

Dynamic mechanical analysis (DMA) is very useful for the structural analysis of viscoelastic materials and their blends via their dynamic moduli and damping characteristics. This dynamic method is extremely sensitive for detecting changes in internal molecular mobility and understanding phase structure and morphology.^{3,4}

Vapor-grown carbon fiber (VGCF) represents a variety of carbon fibers different from pitch-based and polyacrylonitrile-based precursors. VGCF is produced by the thermal decomposition of gas-phase hydrocarbons in the presence of an ultra-fine metallic catalyst of iron.⁵ It has a higher

Correspondence to: M. Sumita (msumita@o.cc.titech.ac.jp).

Journal of Applied Polymer Science, Vol. 82, 3058–3066 (2001)
© 2001 John Wiley & Sons, Inc.

graphitizing nature than the other fibers because its crystal structure is such that carbon hexagonal net planes are well arranged parallel to the fiber axis. Accordingly, it is a new class of carbon fiber that is unique in its very small size, wide surface area, and excellent electrical and thermal conductivities.^{6–8} Otherwise, inorganic alumina reinforcements such as alumina short fiber (ALSF) and inorganic alumina powders (Al_2O_3) are usually used for enhancing strength, wear resistance, and thermal conductivity.⁹

Even though a large amount of work has been carried out on the electric conductivity, mechanical properties, and morphology of VGCF, ALSF, and alumina, it is hard to find documentation, in the areas of vibration and damping, of using them with viscoelastic materials.

In this article, the effects of reinforcement on characteristic vibrational damping properties and viscoelastic behaviors and the relevancy of reinforced ethylene-propylene rubber (EPR) were studied.

EXPERIMENTAL

Materials and Sample Preparation

For the damping matrix, EPR was chosen because it normally has improved impact and tensile properties and is also used for the passive damping control of polymers.¹⁰ JSR EP11 (ethylene content = 52 mol %, density = 0.86 g/cm^3) was obtained from JSR Ltd. (Tokyo, Japan). VGCF (average diameter = $0.2 \mu\text{m}$, average length = $10 \mu\text{m}$, density = 2.0 g/cm^3 ; Showa Denko, Tokyo, Japan), ALSF (mean diameter = $8 \mu\text{m}$, length = $180 \mu\text{m}$, density = 3.1 g/cm^3 , $\text{Al}_2\text{O}_3\text{:SiO}_2 = 72\text{:}28 \text{ wt } \%$ in chemical composition; Mitsubishi

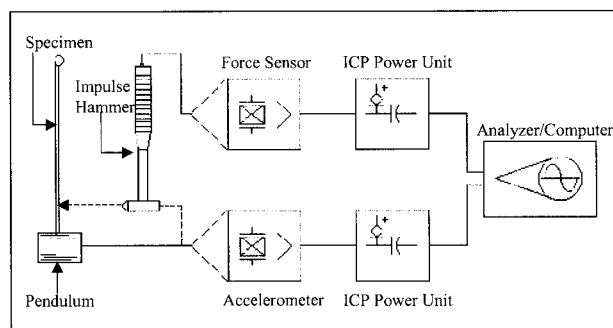


Figure 1 Measuring apparatus for the vibration characteristics of the specimens with the ICP power unit.

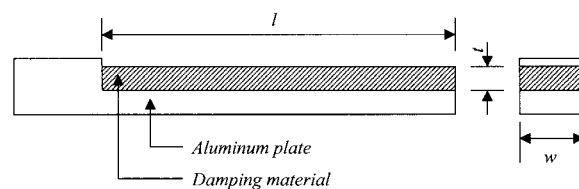


Figure 2 Shape and dimensions of the specimen for the measurement of the vibrational damping loss factor.

Chemical Co., Tokyo, Japan), and alumina powders (average diameter = $10 \mu\text{m}$, density = 3.95 g/cm^3 ; Showa Denko) were used as reinforcement fillers.

The EPR was first melted in a two-roll mill at 120°C , and this was followed by the addition of the fillers to the matrix and mixing for 15 min. The compositions were compression-molded at 140°C for 10 min under a pressure of 20 MPa and finally quenched in liquid nitrogen to obtain sheets 1 mm thick.¹¹

Measurement of the Vibrational Damping Properties

In this study, the impulse technique was used for measuring the damping behaviors of reinforced EPR. The principal components of the apparatus consisted of the test specimen, impulse hammer, force sensor, power unit, analyzer, and accelerometer. The signals from the instrumented force hammer and accelerometer were input into a fast Fourier transform (FFT) analyzer. As a method of data processing for loss factors, the half-power bandwidth method of frequency resolution in the zoom mode on the computer screen was applied to the frequency response function (FRF) curve to evaluate the loss factor.^{12,13} A schematic diagram of the experimental setup for the dynamic measurement of the EPR matrix is shown in Figure 1. All sensors in this system are classified as integrated-circuit-piezoelectric (ICP), low-impedance, and voltage-mode sensors. The ICP power unit supplied constant-current excitation to the sensor over the signal lead, and alternating current coupled the output signal. Many FFT analyzer/computer systems have the ICP power supply built in.

Figure 2 shows the shape and dimensions of the specimen. The width (w) and length (l) of the specimen were 10 and 150 mm, respectively, and we varied the thickness (t) to observe the effects on the damping capacity.^{13,14}

DMA

Dynamic mechanical properties were evaluated with a DVA-200S (Kyoto, Japan). The experiment

was performed in a tension mode with a 0.1% strain amplitude at a frequency of 100 Hz and at temperatures of -70 to 150°C at a heating rate of 5°C/min.

RESULTS AND DISCUSSION

Vibrational Damping Characterization

Damping and dynamic modulus are the most essential properties among all mechanical properties and are very important in the final application of structural materials. In the control of resonant amplitudes of vibration and the extension of the service life of such structures under periodic loads or impacts, damping in the core of a constrained layer plays an important role. Usually, viscoelastic materials as core materials in constrained layers are used for increasing the overall damping characteristics of the structures.

Impulse testing the dynamic behavior of mechanical structures involves striking the test object with a force-instrumented hammer and measuring the resultant motion with an accelerometer or acoustic signature with a microphone. Structures generally respond as rigid or elastic bodies, finite elements, and distributed parameter models conducting stress-strain sound waves. Functional transfer testing of mechanical structures depends on the ratio of the sensitivities, the force sensor to the accelerometer. This ratio can be determined with the hammer to impact a known mass instrumented with the accelerometer to be used.¹⁴ The sensitivity ratio is determined from Newton's law of motion:

$$F = ma \tag{1}$$

where F is the force of impact (N), m is the total mass of the pendulum (kg), and a is the acceleration due to impact (ms^{-2}).

Therefore,

$$F = \frac{V_h}{S_h} = \frac{\text{Signal from Hammer (V)}}{\text{Sensitivity of Hammer (mV/kg)}} \tag{2}$$

and

$$\begin{aligned} ma &= m \frac{V_a}{S_a} \\ &= m \frac{\text{Signal from Accelerometer (V)}}{\text{Sensitivity of Accelerometer (mV/g)}} \tag{3} \end{aligned}$$

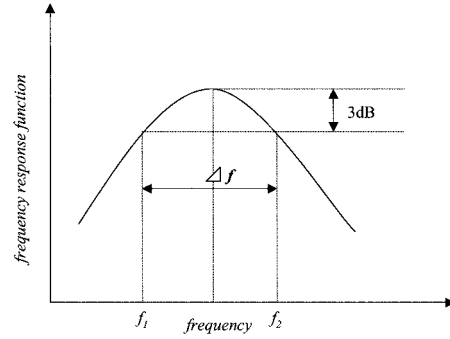


Figure 3 Measuring method for the bandwidth at the half-power points.

Thus,

$$\frac{V_h}{S_h} = m \frac{V_a}{S_a}$$

$$\frac{V_h}{V_a} = m \frac{S_h(\text{mV/kg})}{S_a(\text{mV/g})}$$

$$\text{FRF} = \frac{V_a}{V_h} = \frac{1}{m} \frac{S_a}{S_h} \left(\frac{\text{kg}}{\text{g}} \right) \tag{4}$$

where S_h/S_a is the sensitivity ratio (g/kg).

The vibrational damping loss factors (η_n) of the specimens were determined by the half-power bandwidth method,¹⁴ as shown in Figure 3, which presents a measuring method for the loss factors with respect to the calculated sensitivity ratio at the frequencies of the specimens:

$$\eta_n = \frac{\Delta f}{f_n} = \frac{f_2 - f_1}{f_n} \tag{5}$$

where Δf is the bandwidth at the half-power points; f_2 and f_1 are the right-side and left-side frequencies (Hz) of the half-power band (3dB), respectively; and f_n is the resonant frequency for the n th mode.

Figure 4 shows the measured vibrational damping loss factors of specimens reinforced by given fillers for different impulse frequencies as a function of thickness. To calculate the dissipated energy in a reinforced elastomer, we must accurately evaluate the basic damping loss factors. As an experimental result, the loss factor appears to increase with increasing thickness of the specimen and impulse frequency. For fiber-reinforced EPR, the damping value is higher than those of

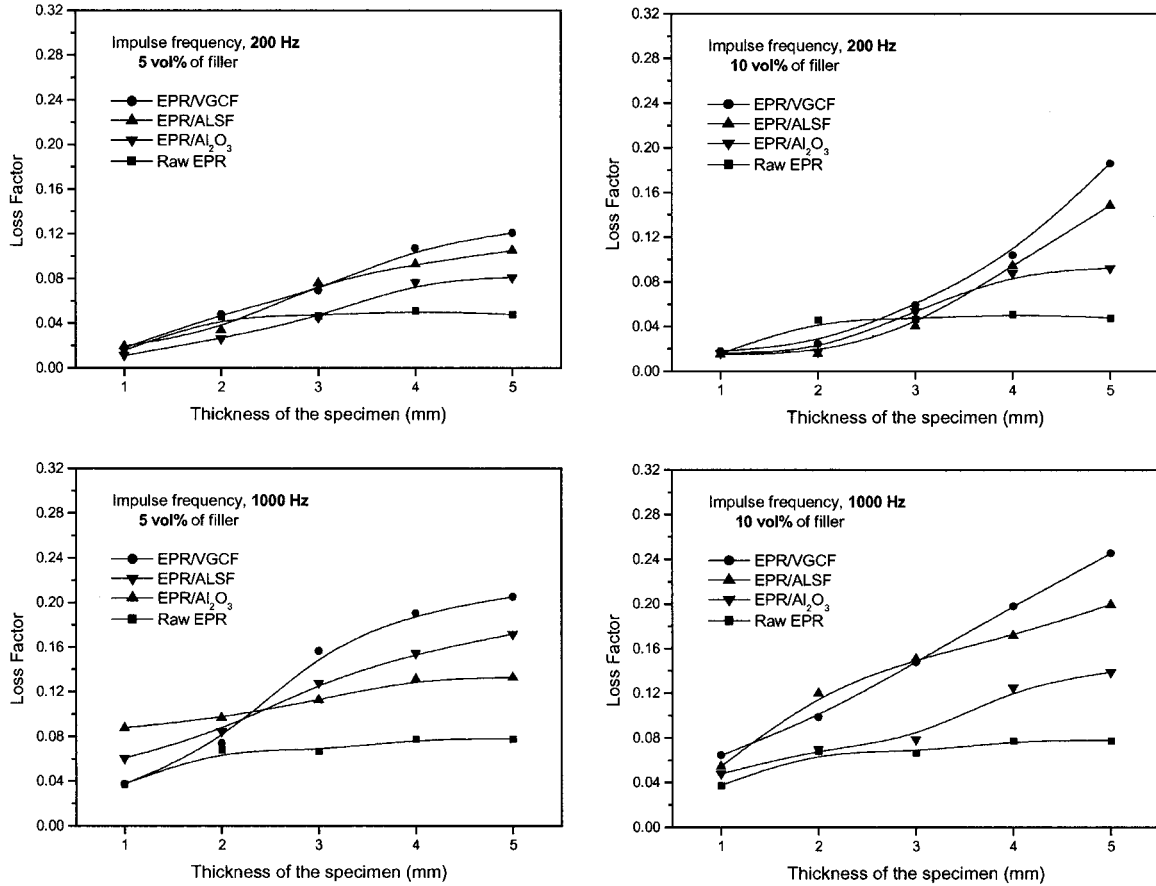


Figure 4 Loss factors of the raw and reinforced EPR specimens at various thicknesses and impulse frequencies.

inorganic alumina particles and raw EPR. In particular, VGCF-reinforced EPR shows the highest damping for specimens greater than 3 mm thick.

Figure 5 shows increased damping capacity under the influence of the sample thickness, filler type, and composition obtained from the loss factor. It can be seen from this figure that with the thickness of the viscoelastic materials and the filler content increasing, higher damping can be achieved in this system. However, it is also evident that this increase in damping is not a linear function of the filler content in the case of alumina.

Material damping allows the conversion of mechanical energy into heat.¹⁴ The energy dissipation occurs through the relaxation, across the specimen, of heat caused by internal friction. For reinforced viscoelastic materials, there are numerous sources of energy dissipation, such as the viscoelastic response of the material constituents, thermoelastic conversion of mechanical energy

into heat, friction at the filler–matrix interface, and stress variations that result from the nonhomogeneous material characteristics of the component.¹⁵

VGCF has the structure and growth mechanism of single-crystal whiskers with a circular cross section and a preferred orientation in which networks of carbon planes are placed parallel to one another along the direction of the fiber axis.¹⁶ The orientational alignment is greater than that of conventional carbon fibers. One of the distinguishing structural features of VGCF is the presence of a hollow tube, about 10 nm or less in diameter, along the fiber axis.⁵ The tube wall is composed of linearly extended single-crystalline-like carbon layers that might account for the higher damping properties and elastic modulus of VGCF.^{5,16,17}

Consequently, it is known that VGCF has a remarkable damping characteristic, that is, an energy dissipation ability due to inherent chemi-

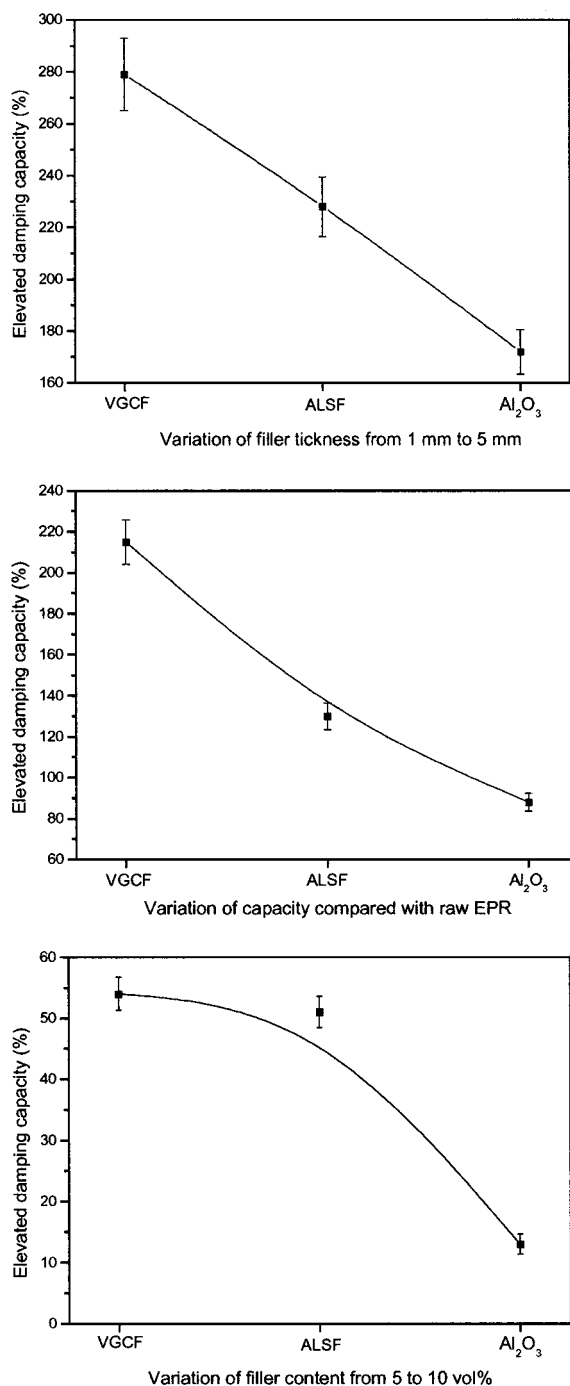


Figure 5 Elevated damping capacity as a function of sample thickness, filler type, and composition.

cal and morphological properties such as carbon-carbon covalent bonds, orientational alignment, and inner hollow tubes.

Viscoelastic Properties

DMA is another thermal analysis technique that can be used to study, in particular, changes in the

short-term storage modulus as a function of temperature and to obtain other information, such as damping characteristics.^{3,4,18}

A real and imaginary component of the modulus can be obtained by resolution of the stress-strain components:^{19,20}

$$\sigma = \epsilon_0 E' \sin(\omega t) + \epsilon_0 E'' \cos(\omega t) \quad (6)$$

where σ is the stress, ϵ_0 is the strain, $E' = (\sigma_0/\epsilon_0)\cos \delta$ is the storage modulus, $E'' = (\sigma_0/\epsilon_0)\sin \delta$ is the loss modulus, and ω is the frequency.

E' is a measure of the recoverable strain energy in a deformed specimen. E'' is related to the dissipation of energy as heat due to the deformation of the material. The ratio E''/E' is the loss tangent $\tan \delta$, which is the ratio of energy lost per cycle to the maximum energy stored per cycle.¹⁷

Figure 6 shows E' as a function of temperature with the filler composition as a parameter. Below the geometric percolation threshold, there are no remarkable modulus deviations with filler content. On the other side, the filler efficiency above the glass-relaxation temperature (ca. -40°C) is drastically high in the case of VGCF, which is known to have a great influence on the reinforcement effect.²¹

E'' and $\tan \delta$ provide information about transformation change and damping in materials.¹⁸ From DMA experiments, the evolution of E'' and $\tan \delta$ curves is also obtained, as shown in Figures 7 and 8, respectively. It is significant that the maximum E'' peaks for VGCF and ALSF are shifted to higher temperatures, and their values increase with increasing fiber content. However, the maximum of the $\tan \delta$ peak for the relaxation near the glass-transition temperature, known as the α relaxation, decreases with increasing filler content. Meanwhile, the alumina-reinforced EPR shows a different behavior, as reported.³ In general, the most intense peak observed for either E'' or $\tan \delta$ in conjunction with a relatively pronounced drop in E' corresponds to the glass transition.²² At this point, local segmental motions appear and a loss peak is presented because of the energy dissipation. On a molecular scale, the glass-relaxation temperature reflects the mobility of the macromolecules in the matrix. An increase in this temperature corresponds to a decrease in the mobility of the chains. This reduction in segmental mobility for short-fiber-reinforced EPR indicates that the reduction in mobility affects a region located near the matrix-substrate inter-

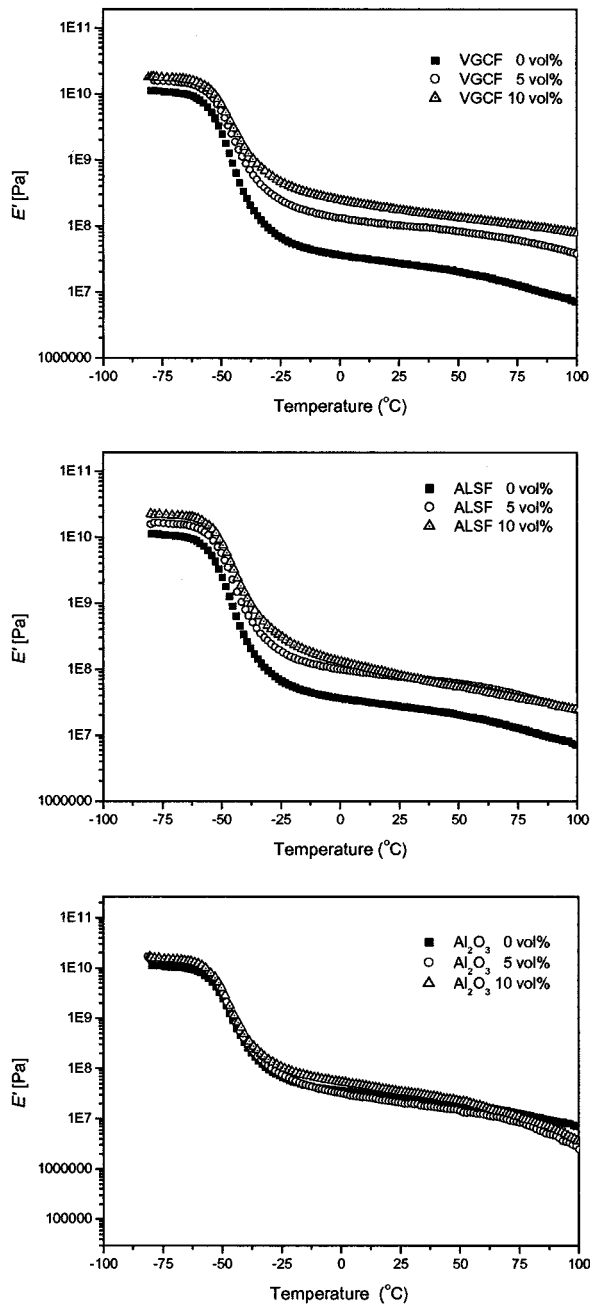


Figure 6 E' measured by DMA as a function of temperature with the filler composition as a parameter.

face. This result suggests the formation of an interphase that exhibits different viscoelastic and damping properties than the inorganic particles.^{23,24} Meanwhile, the inorganic alumina particles show no significant difference in $\tan \delta$ because of a lack of association between EPR and alumina in this system.

Figure 9 shows $\tan \delta$ as a function of E' that resulted from the damping capacity and behav-

iors with the filler composition. With an increase in E' , $\tan \delta$ increased with fiber content; however, alumina-reinforced EPR showed no remarkable shift, in good agreement with the results of Figure 8.

The frequency dependence of $\tan \delta$ versus temperature plots, also obtained from DMA, and the corresponding filler type are shown in Figure 10.

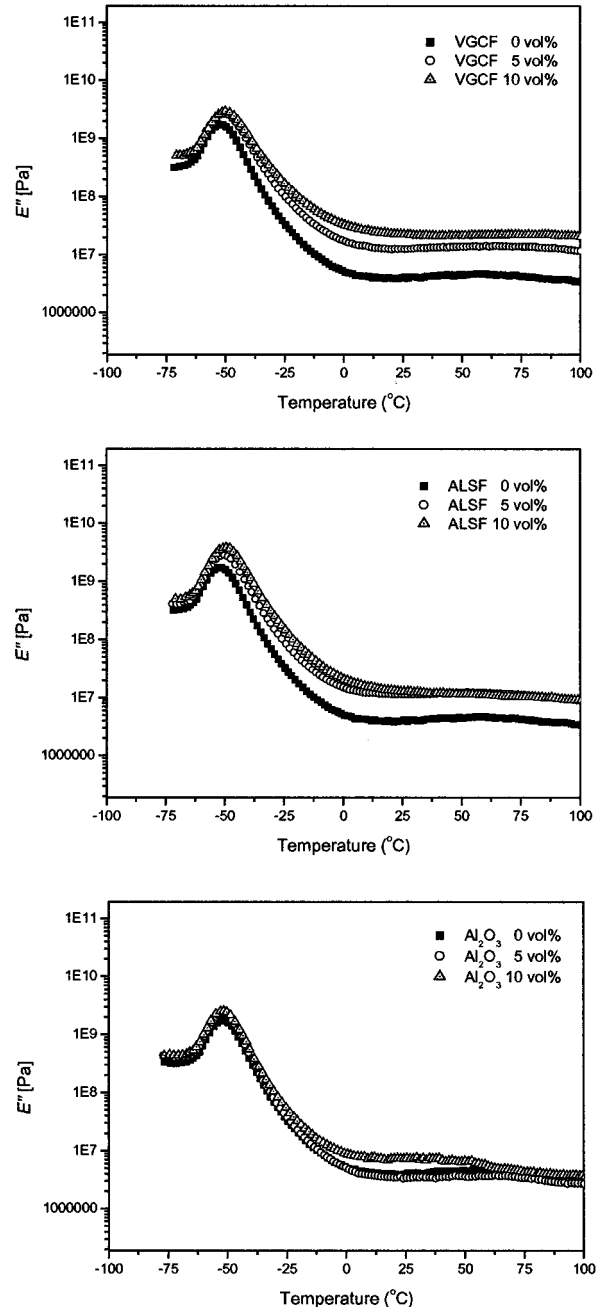


Figure 7 E'' measured by DMA as a function of temperature with the filler composition as a parameter.

The frequency range in this test was varied within 1, 25, 50, and 100 Hz. The temperature relaxation peaks shifted to lower temperatures with increasing frequency for fiber-reinforced EPR. However, $\tan \delta$ increased and shifted to higher temperatures as a function of frequency for the alumina-filled EPR as reported.¹⁵ The high loss factors for the alumina-filled EPR with frequency may be due to the low stiffness and

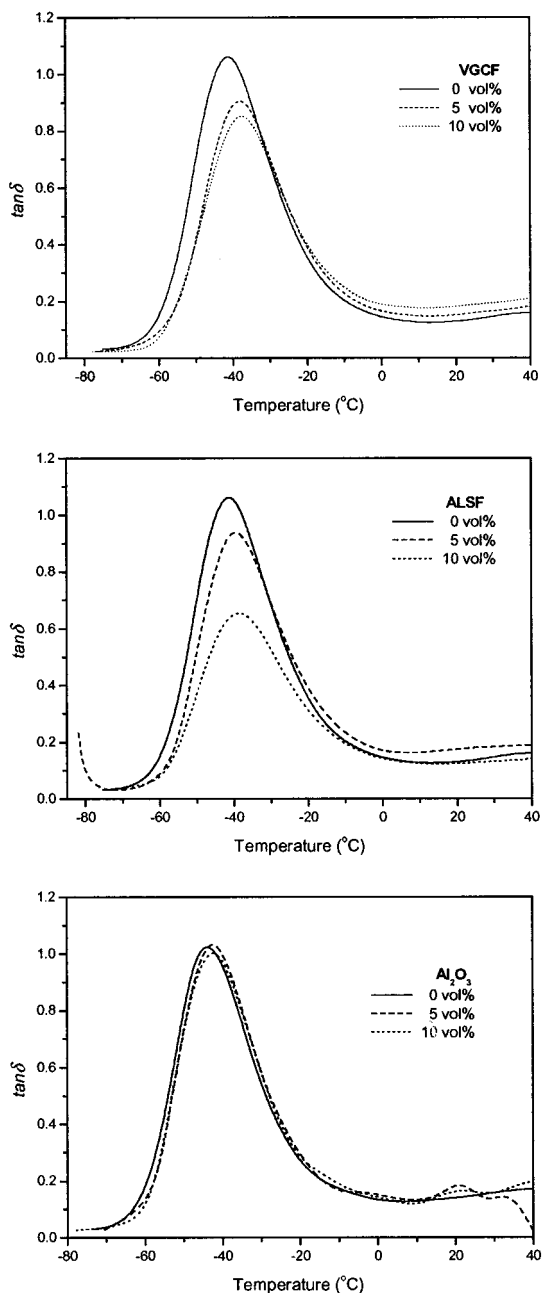


Figure 8 $\tan \delta$ measured by DMA as a function of temperature with the filler composition as a parameter.

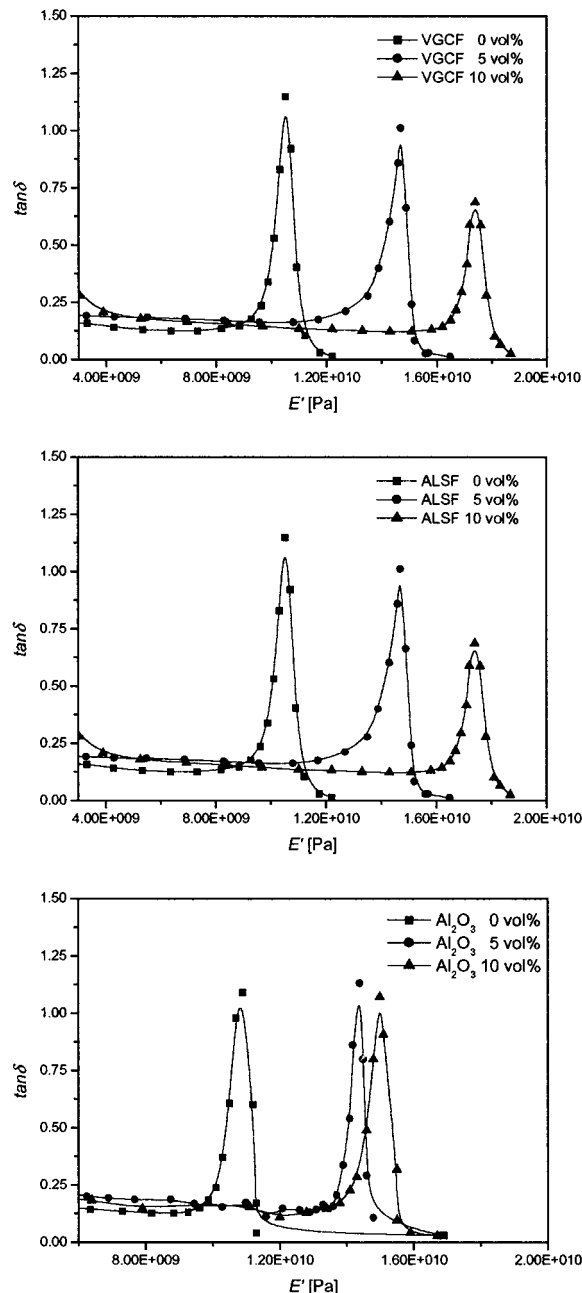


Figure 9 $\tan \delta$ as a function of E' with the filler composition as a parameter.

different damping mechanisms with respect to fiber-filled EPR. The deviations may be the result of structural properties and good compatibility with EPR of the short-fiber-type fillers versus the weak matrix interphase of alumina particles.

Through the DMA experiments, we investigated E' , E'' , and their ratio and the mechanical damping loss factor to evaluate the correspondence between the vibrational damping behaviors

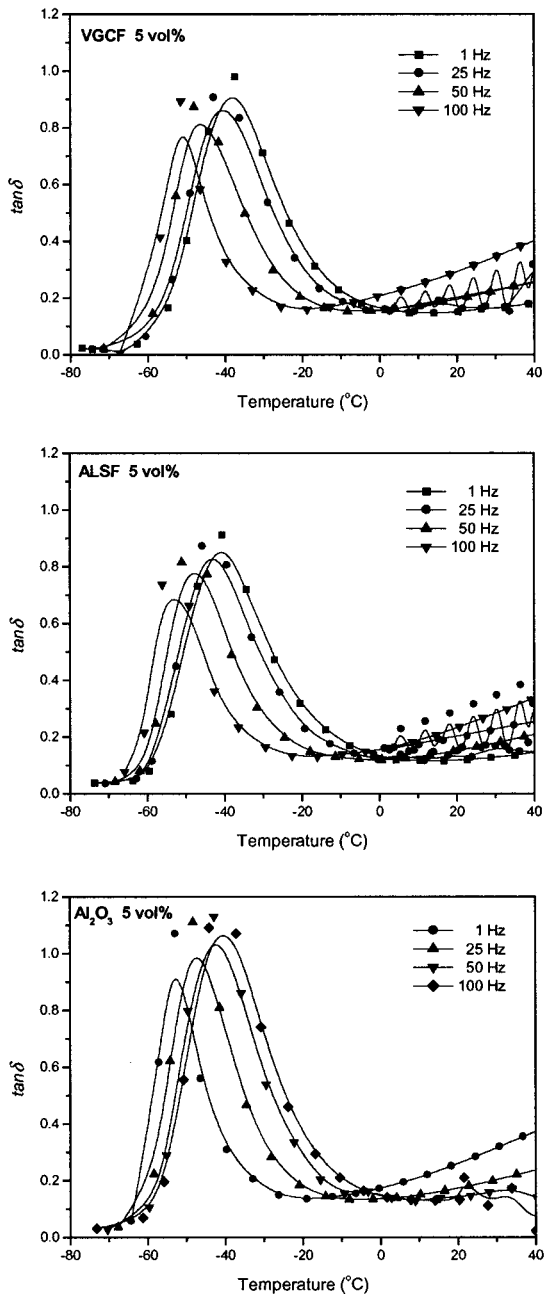


Figure 10 $\tan \delta$ as a function of temperature for various frequencies.

and dynamic mechanical properties. In this work, it is known that the effectiveness of a damping elastomer by reinforcement with microscale fillers depends on the morphology of the blend, such as the shape of the filler type, its size, and the degree and nature of the compatibility between different phases, inherent properties of the filler, and viscoelastic behaviors that are influenced by the reaction temperature, filler content, and frequency.

CONCLUSION

The effects of microscale fillers on the vibrational damping properties and viscoelastic behaviors of EPR were observed with an impulse technique and DMA, respectively. In the experimental results, fiber-reinforced EPR specimens such as VGCF and ALSF showed higher damping capacity than inorganic particles did.

The transition temperature determined by DMA was dependent on not only filler composition but also frequency. In addition to composition and frequency, the mechanical/rheological property used to determine the glass-relaxation temperature also was specified.

In this system, VGCF showed an optimum vibrational damping capacity and reasonable energy dissipation ability; these might have resulted from inherent characteristics, such as the growth mechanism of single-crystal whiskers, which had circular cross sections and preferred orientations; high stiffness; carbon-carbon covalent bonds; inner hollow tubes; and good compatibility with EPR, forming an interphase that dissipated external stress. As a result, VGCF combined good damping properties, which could dissipate external stress, and a reasonable mechanical stiffness.

REFERENCES

1. Saravanam, C.; Ganesan, N.; Ramamuriti, V. *Comput Struct* 2000, 75, 395.
2. Wolfenden, A. *J Mater Sci* 1997, 32, 2275.
3. Wolfenden, A.; Wolla, M. *J Mater Sci* 1989, 24, 3205.
4. Sepe, M. P. *Adv Mater Process* 1992, 4, 32.
5. Endo, M. *CHEMTECH* 1988, 18, 568.
6. Wu, G. Z.; Asai, S.; Sumita, M. *Macromolecules* 1999, 32, 3534.
7. Zhang, C.; Yi, X. S.; Yui, H.; Asai, S.; Sumita, M. *J Appl Polym Sci* 1998, 69, 1813.
8. Katsumata, M.; Endo, M.; Ushijima, H.; Yamashita, H. *J Mater Res* 1994, 9, 841.
9. Mochida, T.; Taya, M.; Lloyd, D. J. *Mater Trans* 1991, 32, 931.
10. Gary, G.; McHugh, J. J. *J Mater Res* 1999, 14, 2871.
11. Zhang, C.; Yi, X. S.; Asai, S.; Sumita, M. *J Mater Sci* 2000, 35, 673.
12. Lee, D. G.; Chang, S. H. *Compos Struct* 1998, 43, 155.
13. Crane, R. M.; Gillespie, J. W. *Compos Sci Technol* 1991, 40, 355.

14. Nashif, A. D.; Jhones, D. I. G.; Henderson, J. P. *Vibration Damping*; Wiley: New York, 1985.
15. Suarez, S. A.; Gibson, R. F.; Deobald, L. R. *Exp Tech* 1984, 8, 19.
16. Ganapathi, M.; Patel, B. P.; Boisse, P.; Polit, O. *Compos B* 1999, 30, 205.
17. Riggs, D. M.; Shuford, R. J.; Lewis, R. W. *Handbook of Composites*; Van Nostrand Reinhold: New York, 1982.
18. Armeniades, C. D.; Baer, E. *Introduction to Polymer Science and Technology*; Wiley Interscience: New York, 1977.
19. Zhang, J.; Perez, R. J.; Lavernia, E. J. *J Mater Sci* 1993, 28, 835.
20. Kwak, G. H.; Park, J. H.; Kim, K. S.; Park, S. J. *Polymer (Korea)* 1999, 23, 427.
21. Sandrade, J.; Auto, A. M.; Kobayashi, Y.; Shibus, Y.; Shirane, K. *Phys A* 1998, 248, 227.
22. Boluk, M. Y.; Schreiber, H. P. *Polym Compos* 1986, 5, 295.
23. Weber, M. E.; Kamal, M. R. *Polym Compos* 1992, 13, 2.
24. Kwak, G. H.; Park, S. J.; Lee, J. R. *J Appl Polym Sci* 2000, 78, 290.